Journal of Peptide Science
J. Peptide Sci. **11**: 3–16 (2005)
Published online 7 July 2004 in Wiley InterScience (www.interscience.wiley.com). DOI: 10.1002/psc.586

JOURNAL OF PEPTIDE SCIENCE

Structural characterization of cyclic kallidin analogues in DMSO by nuclear magnetic resonance and molecular dynamics

ELISABETTA SCHIEVANO, LAURA SILVESTRI, MARINA GOBBO, STEFANO MAMMI, RANIERO ROCCHI and EVARISTO PEGGION*

Department of Chemical Sciences, University of Padova, Via Marzolo 1, 35131 Padova, Italy

Received 1 April 2004; *Accepted 13 April 2004*

Abstract: The conformational properties in DMSO of two head-to-tail cyclic analogues of kallidin ([Lys^0]-bradykinin, KL) as well as those of the corresponding linear peptides were studied by NMR and molecular dynamics (MD) simulations. The modifications in the sequence were introduced at position 6, resulting in the four peptides, [Tyr^6]-KL (**YKL**), [Trp^6]-KL (**WKL**), cyclo-([Tyr^6]-KL) (**YCKL**) and cyclo-([Trp^6]-KL) (**WCKL**).

The linear **WKL** analogue was significantly more potent than kallidin on rat duodenum preparations, whereas **YKL** was significantly less potent. Both cyclic peptides, **YCKL** and **WCKL** displayed similar activity, lower than that of the linear analogues and also of cyclo-KL.

The two linear analogues display high conformational flexibility in DMSO. In the predominant conformer, for both peptides, all three X-Pro bonds adopt a *trans* configuration. Three out of four conformers present in **YCKL** and **WCKL** were completely assigned. The configurations at the X-Pro bonds are the same for the two analogues. All cyclic conformers show a *cis* configuration in at least one X-Pro bond and always opposite configuration for the two consecutive X-Pro bonds.

The NOE-restrained MD calculations resulted in the detection of several elements of secondary structure in each of the conformers. Such elements are described and their possible relevance to biological activity is discussed.

Keywords: bradykinin; kallidin; cyclic analogues; NMR

INTRODUCTION

Kinins are potent bioactive peptides formed by the enzymatic action of kallikreins on endogenous substrates, kininogens [1,2]. The primary structures of mammalian kinins, the nonapeptide bradykinin (BK) and kallidin ([Lys^0]-BK, KL), show a remarkable homology with insect [3], reptile [4] and avian (ornitho) kinins [5]. In fish, the existence of a functioning kallikrein–kinin system has not been unequivocally established yet, although proteolytic cleavage of kininogenin plasma of the rainbow trout *Oncorhynchus mykiss* generates the related peptide [Lys^0, Trp^5, Leu^8]-BK [6].

Kinins are involved in a variety of physiological functions, and are initiators of many pathological processes; they influence the regulation of blood pressure [7] and renal and cardiac functions [1]. They also cause the contraction of the smooth muscle of respiratory and gastrointestinal tracts [7]. BK is implicated in the pathogenesis of hypertension, and is involved in the initiation of pain stimuli [8] and symptoms of inflammation [9], and has also been associated with the symptoms of the common cold [10,11]. In the peripheral nervous system of vertebrates, BK depolarizes nerve cells [1] and, in the insect central nervous system, [Thr^6]-BK blocks the nicotinic synaptic transmission [3]. BK interacts with at least two different types of G-protein-coupled receptors, designated B1 and B2 [12]. Most of the acute and many of the chronic responses to BK are mediated by B2 receptors [13] while some of the chronic responses to BK are mediated by B1 receptors [14].

Because of this wide spectrum of physiological functions, great efforts have been put into the development of BK agonists and antagonists as drugs, and hundreds of compounds have been synthesized and tested.

Despite the substantial amount of structural data obtained from the study of these molecules, the bioactive conformation of BK remains an elusive goal. The conformational properties of kinins and kinin analogues have been studied extensively by various groups, with the aim of determining structure–activity relationships as important steps in structure-based drug design.

Theoretical analyses [15,16] reveal a preference to form a β-turn at the *C*-terminus and the possibility of a bend at the *N*-terminus [17]. The presence of three proline residues, often involved in turns or bends in proteins, can be expected to reduce the conformational freedom of kinin peptides, although both *trans* and *cis* configurations of the X-Pro peptide bonds could be populated.

* Correspondence to: Evaristo Peggion, Department of Chemical Sciences, University of Padova, Via Marzolo 1, 35131 Padova, Italy; e-mail: evaristo.peggion@unipd.it

The general conclusion of extensive spectroscopic studies of kinins and kinin analogues is that in aqueous solution they possess a high degree of flexibility which could account for the variety of biological properties of these peptides [18]. Specifically, less than 10% of *cis* configuration was observed, the presence of the three Pro residues notwithstanding [19–21]. No backbone hydrogen bonding was detected for BK in water, despite the predicted high probability for β-turns in the Pro-Pro-Gly-Phe and in the Ser-Pro-Phe-Arg sequences. Few elements of ordered structure were found in non-aqueous media. A *C*-terminal β-turn was detected in DMSO [13,22–27], in SDS micelles [13,24,28–30], and in dioxane/water solvent mixture [31] and an *N*-terminal turn was also detected in trifluoroethanol/water 95 : 5 [32] and in methanol/water 60 : 40 [33].

Among several strategies to reduce the conformational freedom of bioactive peptides, cyclization has been frequently used. In the case of BK, this approach was suggested by the observation that the formation of two β-turns at either end of the molecule could induce a pseudo-cyclic structure which might be of biological relevance [13,33–35]. Since the initial investigation of Chipens [35,36], several head-to-tail [37–40] and side-chain [41,42] cyclic analogues of kinins have been synthesized and tested for their activity on different organs and tissues. In general, these cyclic analogues behave as poor agonists, with the exception of some head-to-tail cyclic kinins with a 33-atom ring which showed a similar or slightly higher potency compared with that of linear BK [3,23,24,35–37,40,43].

Most of the cyclic analogues exist in solution as an ensemble of conformers in equilibrium. Conformational investigations have been carried out on some of the smaller-sized cyclic analogues [23,44] in spite of their low potency of smooth muscle, because they specifically recognize B2 receptors [38], and could therefore help to identify the structural requirements for agonistic activity and receptor specificity.

Recently, the synthesis and the pharmacological properties of linear and cyclic analogues of KL in which the Phe^6 residue was replaced by either Tyr or Trp were reported [38]. These substitutions were chosen in light of the involvement of Phe^6 in binding to the receptor, demonstrated by previous studies on kinins. The potent BK antagonist HOE 140 contains and β-(2-thienyl)-alanine in this position [45]. On isolated rat duodenum preparations, the linear Trp^6-KL analogue (**WKL**) was significantly more potent than the parent peptide, whereas Tyr^6-KL (**YKL**) was significantly less potent (Table 1), suggesting that the characteristics of the central aromatic residue in kallidin are critical for positive interaction with a hydrophobic pocket within the receptor [13,46]. This feature was lost in the corresponding cyclic peptides, cyclo-([Tyr^6]-KL) (**YCKL**) and cyclo-([Trp^6]-KL) (**WCKL**), which display similar activity, lower than that of the linear analogues and also of cyclo-KL [32].

The present paper reports the results of conformational studies in DMSO, by NMR and MD simulations, of the cyclic analogues **YCKL** and **WCKL** as well as on those of the corresponding linear peptides, **YKL** and **WKL**. Structural studies on BK analogues in DMSO carried out by various research groups [13,22–27] revealed that in this solvent medium the peptide conformations are often similar to those detected in membrane-mimetic environments such as SDS or DPC micelles [13,24,27,34]. These results indicate that the conformational preferences of these peptides are not strongly dependent on the environment, and justify a structural study in a solvent which is very far from the physiological medium. The constraints present in a cyclic decapeptide containing three prolines should sufficiently reduce the available conformational space so that relevant biological considerations can be drawn from such structural studies.

MATERIALS AND METHODS

The synthesis of the peptides has been reported elsewhere [38].

Nuclear Magnetic Resonance

NMR spectra were recorded on a Bruker DMX spectrometer operating at 600 MHz. Peptides were dissolved at 6 mM concentration in deuterated dimethylsulfoxide (DMSO-d_6).

All spectra were acquired at 298 K. Chemical shifts are reported relative to tetramethylsilane (TMS) as internal standard.

For sequence-specific assignments, DQF-COSY [47], CLEAN-TOCSY [48,49], NOESY [50,51] and ROESY [52] spectra were used. The mixing time for the CLEAN-TOCSY spectra was 70 ms utilizing a spin-locking field of 10 kHz; the mixing time for NOESY and ROESY experiments was 150 ms.

Table 1 Sequence and Biological Activity of the Peptides Described in this Work.

Peptide	Sequence	EC_{50} (M)
KL	H-Lys-Arg-Pro-Pro-Gly-Phe-Ser-Pro-Phe-Arg-OH	2.9×10^{-10}
YKL	H-Lys-Arg-Pro-Pro-Gly-Tyr-Ser-Pro-Phe-Arg-OH	8.7×10^{-8}
WKL	H-Lys-Arg-Pro-Pro-Gly-Trp-Ser-Pro-Phe-Arg-OH	1.1×10^{-12}
CKL	cyclo(-Lys-Arg-Pro-Pro-Gly-Phe-Ser-Pro-Phe-Arg-)	2.3×10^{-8}
YCKL	cyclo(-Lys-Arg-Pro-Pro-Gly-Tyr-Ser-Pro-Phe-Arg-)	3×10^{-7}
WCKL	cyclo(-Lys-Arg-Pro-Pro-Gly-Trp-Ser-Pro-Phe-Arg-)	1×10^{-6}

In NOESY spectra, the mixing period was varied randomly by ±10% to reduce zero quantum coherence contributions. ROESY spectra were obtained with a single spin-locking pulse of $\gamma B_2/2\pi$ of 3.3 kHz.

All data were collected with 256–512 experiments of 2K data points and 32–240 scans. Prior to Fourier transformation, the time domain data were multiplied by shifted sine-bell functions in the F1 dimension and gaussian functions in F2; zero filling to 4K × 1K real points was employed to increase the digital resolution. Fifth-order polynomial baseline corrections were applied in the $\omega 2$ dimension after transformation. The spectra were acquired in the phase-sensitive manner using the time proportional phase incrementation method (TPPI) [53,54].

^{1}H chemical shift assignments were obtained using the standard procedure developed by Wüthrich [55]. DQF-COSY and TOCSY spectra were used to identify the spin systems of the residues. To establish the sequential assignments, NOESY spectra were analysed.

In order to investigate the participation of the polar hydrogen atoms in hydrogen bonds, temperature coefficients of the amide proton chemical shifts were derived from CLEAN-TOCSY spectra at different temperatures in the range 298–313 K. In the case of **WCKL,** NOESY spectra at different temperatures were also used to resolve some NH-CαH peak overlap.

Distinction between *trans* and *cis* X-Pro bonds was achieved by means of heteronuclear [^{13}C-^{1}H] HMQC-TOCSY [56] experiments with 220 experiments of 2K data points, 320 scans and a spectral window of 50 ppm in $\omega 1$. The signals from protons not directly attached to a ^{13}C nucleus were suppressed by the application of a BIRD [57] pulse train, while ^{13}C decoupling during acquisition was achieved with a GARP [58] sequence. The spin locking sequence, MLEV-17, was cycled for a total mixing time of 50 ms.

Inter-residue and intra-residue NOEs (determined only for the cyclic peptides, see below) were converted to distance information using the AURELIA [59] software. Appropriate peaks between methylene protons which are at a fixed distance of 1.78 Å were chosen for distance calibration: for **WCKL**, Gly^5 $H_\alpha/H_{\alpha'}$, was selected for conformer I, Pro^8 $H_\gamma/H_{\gamma'}$, for conformer II and Phe^9 $H_\beta/H_{\beta'}$, for conformer III; for **YCKL,** Pro^8 $H_\beta/H_{\beta'}$, was chosen for conformers I and II and Pro^3 $H_\beta/H_{\beta'}$, for conformer III. Distances were adjusted by ±10% to produce upper and lower distance restraints. Pseudoatoms were used for aromatic rings, methyl groups and identical methylene protons with the appropriate correction of the distance restraint following standard procedures [60].

Structure Determination

The XPLOR software, version 3.0 [61], was used for structure determination of each peptide. The structure calculations started from a template structure with randomized ϕ and ψ angles and extended side chains. The structure of all the conformers was regularized by distance geometry (DG) with the metric matrix method followed by restrained molecular dynamics using a simulated annealing protocol with a force constant of 50 kcal/mol for the NOE-derived distance restraints. The SA procedure was the following: 16 ps of dynamics at 1500 K (8000 cycles, in 2 fs steps); cooling from 1500 K to 100 K in 20 ps, in 50 K decrements (10 000 cycles, in 2 fs steps).

The SA procedure, in which the weights of NOEs and non-bonded terms were gradually increased, was followed by 200 cycles of energy minimization. The refinement stage consisted of two steps: (1) the system was cooled from 1000 K to 100 K in 50 K decrements (10 000 cycles, in 1 fs steps) followed by 200 cycles of energy minimization. (2) Cooling from 501 K to 1 K in 20 K decrements (10 000 cycles, in 1 fs steps) and then the energy of each refined structure was minimized for 200 cycles to yield a final structure.

The structures generated by XPLOR were visualized and analysed with the software MOLMOL [62] and INSIGHT.

RESULTS

NMR Results

For all the peptides studied, the number of signals in the NH-CαH region exceeds by far the number expected for a single conformer. Moreover, both positive and negative cross-peaks are present in the ROESY spectra. These results are clear evidence that the peptides exist as an ensemble of conformers slowly interconverting on the NMR time scale. These conformers differ in the *cis-trans* configuration at the X-Pro peptide bonds.

The three X-Pro bonds could lead in principle to eight interconverting conformers. In the two linear analogues, only the most abundant conformer exhibited a complete spin system for all residues and was completely assigned. For both cyclic peptides, only four sets of peaks were observed in our experimental conditions and only three of such conformers showed complete spin systems for all 10 residues and were completely assigned. The assignment of proton resonances for each conformer of the four peptides is reported in Tables 2–5.

For the two linear analogues, the most populated conformer is present in a ratio of 8 : 1 to the second most populated one, based on the integrated intensities in the 1D spectra. In the predominant conformers, the X-Pro bonds are all in a *trans* configuration as indicated by the presence of diagnostic cross peaks between the δ protons of the proline residues and the α protons of the preceding amino acids in the NOESY spectra (data not shown). In these spectra, only intra-residue and sequential cross peaks were present. The complete absence of medium range correlations is a clear indication that both peptides adopt a disordered conformation in solution. For this reason, structure calculations were deemed unnecessary for the two linear peptides and were therefore not performed.

The amide to aliphatic correlation regions of NOESY spectra of the cyclic peptides are shown in Figures 1 and 2. The resonance assignment of the three conformers was obtained by comparing the NOESY and the ROESY spectra in which the exchange between conformers gave rise to positive peaks. The relative amounts of the three conformers were obtained from the volume of Pro^8 H_β/H_γ cross peaks in the TOCSY spectra. For **WCKL,** a population of I : II : III = 3.5 : 3 : 1

Table 2 ^{1}H Chemical Shifts (ppm) Relative to TMS for **WCKL**, 6 mM, in DMSO-d_6. **a**, conformer I; **b**, conformer II, **c**, conformer III

AA	NH	α	β	γ	Others	$\Delta\delta/\Delta T$ (ppb/K)
a Conformer I						
Lys[1]	8.34	4.14	1.57; 1.73	1.34	δ: 1.52 ε: 2.80	−2.00
Arg[2]	7.41	4.54	1.82; 1.51	1.51	δ: 3.11 ε: 7.70	−3.22
Pro[3]		4.33	1.68; 2.27	1.68; 1.87	δ: 3.49; 3.66	
Pro[4]		4.50	1.95; 2.10	1.74	δ: 3.38	
Gly[5]	8.41	3.66; 3.93				−2.10
Trp[6]	8.35	4.60	2.98; 3.18		H2: 7.14 H4: 7.50 H5: 6.97 H6: 7.07 H7: 7.29 NH: 10.85	−5.34
Ser[7]	7.76	4.62	3.50; 3.85		OH: 6.10	−8.32
Pro[8]		4.16	1.27; 1.92	1.37; 1.70	δ: 3.61; 3.67	
Phe[9]	7.67	4.38	2.63; 3.26		Ar: 7.15	−3.12
Arg[10]	7.31	4.22	1.66; 1.78	1.35; 1.51	δ: 3.03 εNH: 7.32	−1.46
b Conformer II						
Lys[1]	8.60	4.11	1.55; 1.77	1.34	δ: 1.52 ε: 2.77	−3.36
Arg[2]	7.16	4.56	1.50; 1.72	1.46	δ: 3.16; ε: 7.30	−0.34
Pro[3]		4.33	1.68; 2.27	1.68; 1.87	δ: 3.73; 3.49	
Pro[4]		4.50	1.95; 2.10	1.74	δ: 3.38	
Gly[5]	8.47	3.48; 3.90				−3.62
Trp[6]	8.10	4.89	2.95; 3.23		H2: 7.62, H4: 7.68 H5: 7.00, H6: 7.07 H7: 7.29, NH: 10.88	−5.52
Ser[7]	8.92	4.44	3.67		OH: 5.33	−5.26
Pro[8]		4.79	1.70; 2.03	0.66; 1.55	δ: 2.80; 3.27	
Phe[9]	7.99	4.26	3.18		Ar: 7.22	−1.56
Arg[10]	7.48	4.42	1.27; 1.85	1.54	δ: 3.11 ε: 7.48	0.98
c Conformer III						
Lys[1]	7.93	4.20	1.53; 1.64	1.25	δ: 1.53 ε: 2.76	−1.62
Arg[2]	7.70	4.34	1.52; 1.82	1.34	δ: 3.1; ε: —	−5.60
Pro[3]		4.87	2.27; 1.98	—	δ: 3.37	
Pro[4]		4.27	1.79; 2.14	1.88; 2.02	δ: 3.72	
Gly[5]	8.01	3.63;3.71				−2.96
Trp[6]	8.34	4.45	2.89; 3.28		H2: 7.09, H4: 7.45 NH: 10.84	−6.18
Ser[7]	7.49	4.72	3.56; 3.84		OH: 5.95	−4.20
Pro[8]		4.25	1.73; 1.87	1.27; 1.39	δ: 3.61	
Phe[9]	7.60	4.41	2.66; 3.19		Ar: 7.19	−1.64
Arg[10]	7.75	4.31	1.51	—	δ: 3.12 ε: 7.46	−4.34

was estimated, while for **YCKL** the ratio was I : II : III = 4 : 3 : 1.

The aliphatic regions of the NOESY spectra are reported in Figures 3 and 4. The exchange peaks in the αH regions for both peptides are clearly evident. For both peptides, these exchange peaks (identified as such in the ROESY spectra) involved only conformers I and II, indicating that they are in fast equilibrium. The absence of exchange peaks involving the third conformer indicates that its interconversion with the other two is slow on the NMR time scale.

The configuration at each X-Pro bond was determined measuring the difference in chemical shift between $^{13}C_\beta$ and $^{13}C_\gamma$ of the proline residues: a difference of about 3 ppm characterizes a *trans* bond while a difference of 10 ppm is typical of a *cis* bond [63,64]. The HMQC-TOCSY experiment is particularly suited for this analysis. As an example, a region of such spectrum obtained for **YCKL** is reported in Figure 5. The X-Pro bond configurations of the three conformers are reported in Table 6. The same configurations were found for both cyclic peptides. At least one *cis* X-Pro

Table 3 ^{1}H Chemical Shifts (ppm) Relative to TMS for **YCKL**, 6 mM, in DMSO-d_6. **a**, conformer I; **b**, conformer II, **c**, conformer III

AA	NH	α	β	γ	Others	$\Delta\delta/\Delta T$ (ppb/K)
a Conformer I						
Lys[1]	8.32	4.15	1.56–1.75	1.34	δ: 1.54 ε: 2.77	−1.84
Arg[2]	7.41	4.55	1.49; 1.81	1.50	δ: 3.07; 3.12 ε: 7.65	−3.98
Pro[3]		4.31	1.69; 2.27	1.87	δ: 3.49; 3.68	
Pro[4]		4.48	1.94; 2.12	1.76	δ: 3.37	
Gly[5]	8.41	3.61; 3.91				−2.18
Tyr[6]	8.29	4.48	2.68; 2.91		H2, H6: 6.99	−5.68
					H3, H5: 6.63	
Ser[7]	7.80	4.62	3.52; 3.90		OH: 6.04	−8.32
Pro[8]		4.17	1.26; 1.93	1.38; 1.70	δ: 3.62	
Phe[9]	7.66	4.39	2.64; 3.25		H2, H6: 7.28	−3.30
					H3,H4, H5: 7.16	
Arg[10]	7.35	4.23	1.64; 1.77	1.38; 1.51	δ: 3.04 ε: 7.30	−2.36
b Conformer II						
Lys[1]	8.56	4.10	1.56; 1.75	1.34	δ: 1.54 ε: 2.78	−3.38
Arg[2]	7.14	4.56	1.43; 1.72	1.49	δ: 3.07; 3.13 ε: 7.30	−0.30
Pro[3]		4.28	1.69; 2.27	1.87; 1.91	δ: 3.49; 3.72	
Pro[4]		4.48	1.94; 2.12	1.76	δ: 3.37	
Gly[5]	8.46	3.45; 3.95				−3.52
Tyr[6]	8.06	4.75	2.63; 2.99		H^2, H^6: 7.09	−6.14
					H^3, H^5: 6.65	
Ser[7]	8.84	4.43	3.65		OH: 5.32	−5.06
Pro[8]		4.76	1.69; 2.01	0.64	δ: 2.76; 3.24	
Phe[9]	7.90	4.26	3.18		H^2, H^6: 7.23	−1.58
					H^3, H^4, H^5: 7.15	
Arg[10]	7.46	4.34	1.24; 1.83	1.51; 1.67	δ: 3.23 ε: 7.30	−0.24
c Conformer III						
Lys[1]	7.91	4.21	1.46; 1.53	1.23; 1.27	δ: 1.52 ε: 2.75	−0.82
Arg[2]	7.70	4.33	1.46; 1.65	1.34	δ: 3.07 ε: 7.19	−6.82
Pro[3]		4.87	1.28; 2.01	1.66	δ: 3.37	
Pro[4]		4.26	1.80; 2.13	1.90; 2.03	δ: 3.53; 3.72	
Gly[5]	8.03	3.60; 3.68				−3.74
Tyr[6]	8.29	4.31	2.63; 3.02		H2, H6: 7.00	−7.16
					H3, H5: 6.63 OH: 9.21	
Ser[7]	7.46	4.69	3.54; 3.83		OH: 5.93	−4.30
Pro[8]		4.25	1.39; 1.87	1.25; 1.26	δ: 3.58	
Phe[9]	7.58	4.34	2.66; 3.18		Ar: 7.19	−2.74
Arg[10]	7.72	4.31	1.62; 1.81	—	δ: 3.10 ε: 7.46	−4.02

bond was observed in each conformer and the all-*trans* conformer was not present in detectable amounts. This indicates a clear difference in the conformational preferences of the linear and the cyclic analogues and shows that cyclization indeed has a significant effect on the energy of the available structures. Assignment of the diagnostic correlations in the NOESY spectra confirmed these results. The $\alpha_X \rightarrow \delta_{Pro}$ cross peak was present in every case of a *trans* bond, and the $\alpha_X \rightarrow \alpha_{Pro}$ cross peak was present in almost all cases of *cis* bonds. The $\alpha_X \rightarrow \alpha_{Pro}$ cross-peak between Pro[3]-Pro[4] in conformer I of **WCKL** was obscured by overlap. The configuration of the three X-Pro bonds accounts for the fact that only conformers I and II show exchange cross peaks. In fact, only the peptide bond between Ser[7] and Pro[8] has a different configuration in these two conformers. On the other hand, two peptide bonds need to change their configuration to go from conformer III to either conformer I or II. This double jump requires much more energy and it is not observed in the NMR time scale.

The intra-residue, sequential and medium-range NOESY connectivities observed for all conformers are summarized in Figures 6a and 6b.

Table 4 ^{1}H Chemical Shifts (ppm) Relative to TMS for **YKL**, 3 mM, in DMSO-d_6

AA	NH	α	β	γ	Others
Lys[1]	8.10	3.80	1.66	1.32	δ: 1.51; ε: 2.74 NH_2: 7.74
Arg[2]	8.62	4.49	1.55; 1.71	1.55	δ: 3.09 NHε: 7.64
Pro[3]		4.55	1.85; 2.16	1.91	δ: 3.50; 3.60
Pro[4]		4.24	2.01	1.82	δ: 3.58
Gly[5]	7.86	3.64			
Tyr[6]	7.85	4.48	2.63; 2.83		H2, H6: 6.77 H3, H5: 6.71 OH: 9.18
Ser[7]	8.23	4.57	3.62		OH: 5.33
Pro[8]		4.30	1.62; 1.88	1.42; 1.70	δ: 3.49
Phe[9]	7.68	4.54	2.72; 3.08		Ar: 7.20
Arg[10]	8.10	4.20	1.64; 1.78	—	δ: 3.12; NHε: 7.55

Table 5 ^{1}H Chemical Shifts (ppm) Relative to TMS for **WKL**, 3 mM, in DMSO-d_6

AA	NH	α	β	γ	Others
Lys[1]		3.79	1.66	1.32	δ: 1.51; ε: 2.73 NH_2: 7.76
Arg[2]	8.63	4.47	1.56; 1.71	1.30	δ: 3.09 NHε: 7.68
Pro[3]		4.53	1.82; 2.14	1.83	δ: 3.46; 3.67
Pro[4]		4.26	1.82; 1.99	1.80	δ: 3.58
Gly[5]	8.01	3.66			
Trp[6]	7.88	4.60	2.92; 3.85		H2: 7.10; H4: 7.54; H5: 6.93; H6: 7.04; H7: 7.30 NH: 10.81
Ser[7]	8.23	4.58	3.63		OH: 5.35
Pro[8]		4.30	1.61; 1.86	1.39; 1.61	δ: 3.44, 3.58
Phe[9]	7.67	4.55	2.72; 3.08		Ar: 7.24
Arg[10]	8.11	4.20	1.64; 1.78	—	δ: 3.13; NHε: 7.56

Structure Calculations

The derivation of distances from the integration of NOESY cross peaks is complicated by the presence of exchange peaks [65]. In fact, during the mixing time of NOESY experiment, a generic (A,X) cross peak could build intensity not only from the direct dipolar interaction but also from chemical exchange $A \rightarrow A'$, followed by $A' \rightarrow X'$ dipolar interaction and $X' \rightarrow X$ exchange. In our case, this contribution can be neglected safely because no cross peak of the type (A,X′) was observed.

From XPLOR simulations, 150 structures for each conformer were generated. In all cases, the structures fulfilling the experimental NOEs with distance violations not greater than 0.5 Å and with lower total energy values were selected. The number of NOE restraints utilized for MD calculations is given in Table 7. Typically, between 40 and 50 structures were analysed.

Tables 8 and 9 summarize the backbone dihedral angles calculated for the three conformers of both peptides as well as their order parameter, S; a small value of S indicates disordered structures whereas the S value is 1 when the angle is the same in all structures [66]. In some cases, few residues are not well defined due to high dispersion of the ϕ and ψ angles and the calculation of their average value, reported in Tables 8 and 9, was obtained excluding the structures in which that particular angle differs more than 3σ from the average.

Conformers I. 41 and 43 structures were selected for **WCKL** and **YCKL**, respectively. Only short-range NOEs were found. The lack of intra-annular NOEs is an indication that in spite of the constraints due to the cyclic structure, a certain degree of flexibility is present in both peptides. The ϕ and ψ angles are not very different in the two peptides; the statistical values are very similar and a structural comparison is possible

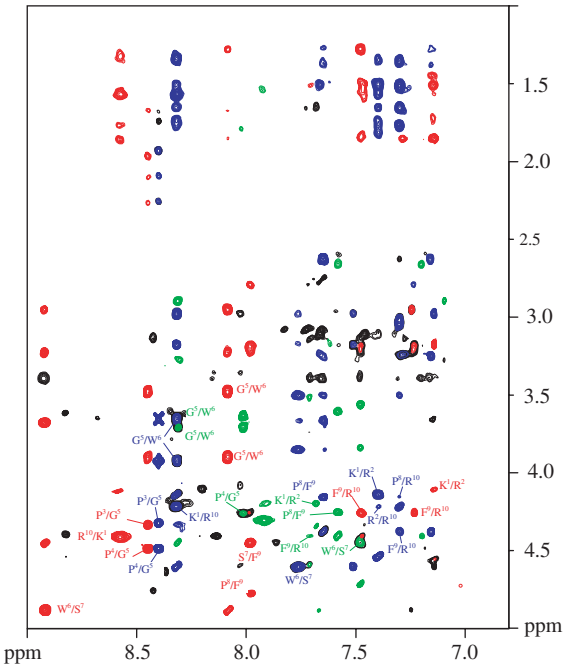

Figure 1 Amide to aliphatic correlation region of the NOESY spectrum at 600 MHz of a 6 mM solution of **WCKL** in DMSO-d_6, T = 298 K, τ_{mix} = 150 ms. The assignment of the three main conformers is shown in different colours: blue, conformer I; red, conformer II; green, conformer III.

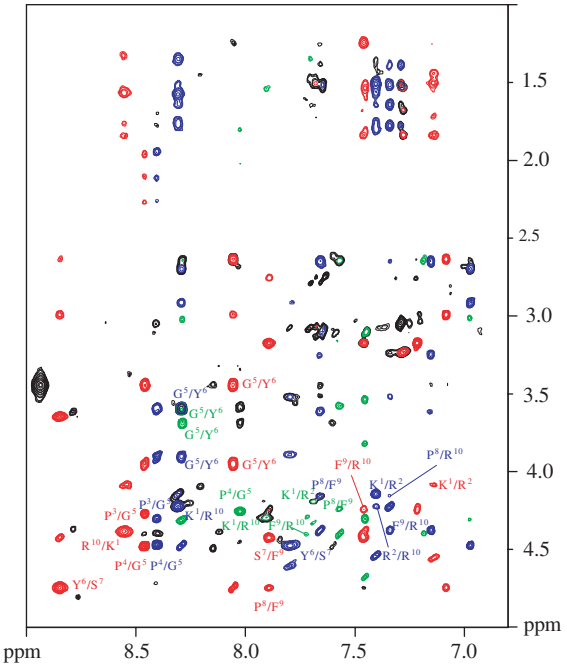

Figure 2 Amide to aliphatic correlation region of the NOESY spectrum at 600 MHz of a 6 mM solution of **YCKL** in DMSO-d_6, T = 298 K, τ_{mix} = 150 ms. The assignment of the three main conformers is shown in different colours: blue, conformer I; red, conformer II; green, conformer III.

(Table 10). In both cases, a high dispersion of the ϕ values of Arg^2 and Arg^{10} and of the ϕ and ψ values

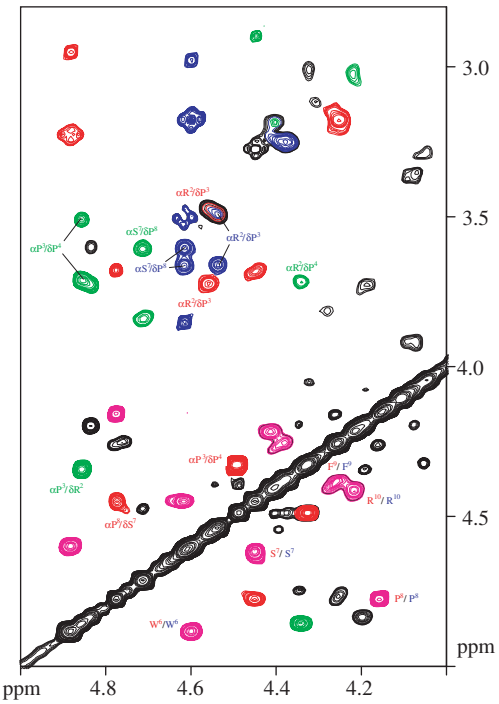

Figure 3 Aliphatic region of the NOESY spectrum at 600 MHz of a 6 mM solution of **WCKL** in DMSO-d_6, T = 298 K, τ_{mix} = 150 ms. The peaks are colour-coded as follows: blue, conformer I; red, conformer II; green, conformer III; magenta, exchange peaks (assigned from ROESY spectra).

of Gly^5 and Ser^7 can be observed from the high value of the corresponding standard deviations and from the low value of the order parameter (Tables 8a and 9a). In the case of **YCKL,** also the ϕ angle of Tyr^6 is not well defined.

Analysis of the backbone dihedral angles shows the possibility of a polyproline II structure in position 2–3 and of a type-I β-turn in position 8–9 for each peptide. The overlay of two representative structures for conformer I of the two peptides is reported in Figure 7.

The hydrogen bonds present in the calculated structures were identified utilizing the appropriate algorithm of MOLMOL: in 76% of the structures of this conformer of **WCKL** and in 100% of the structures of **YCKL** only one H-bond between NH(10) and CO(7) is present, in line with the observation of a type-I β-turn around residues 8–9.

This result is in agreement with the low temperature coefficient of the amide proton resonance of Arg^{10} for both peptides (Tables 2 and 3).

Conformers II. 43 structures were selected for **WCKL** and 45 for **YCKL**. The same NOE pattern was found for both conformers, and also structure calculations yielded very similar results.

The average ϕ and ψ dihedral angles define for both peptides a type-VIb β-turn between Pro^3 and Pro^4 and a type-VIa β-turn between Ser^7 and Pro^8. These types of turns are induced by the presence of a *cis* peptide

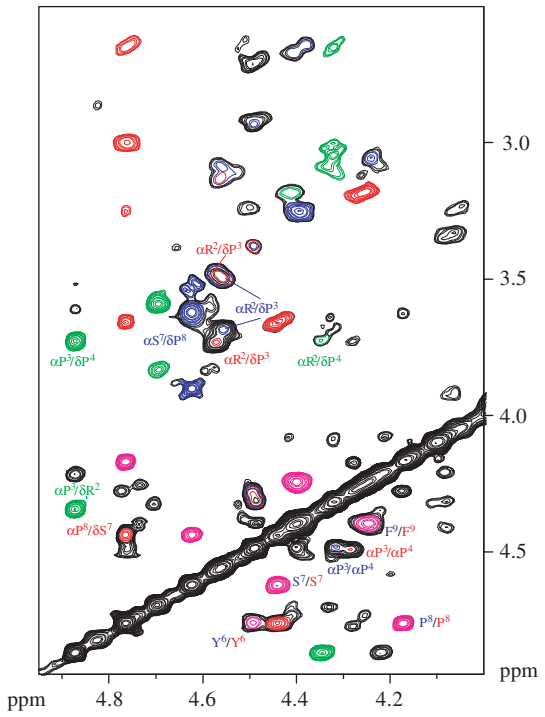

Figure 4 Aliphatic region of the NOESY spectrum at 600 MHz of a 6 mM solution of **YCKL** in DMSO-d_6, T = 298 K, τ_{mix} = 150 ms. The peaks are colour-coded as follows: blue, conformer I; red, conformer II; green, conformer III; magenta, exchange peaks (assigned from ROESY spectra).

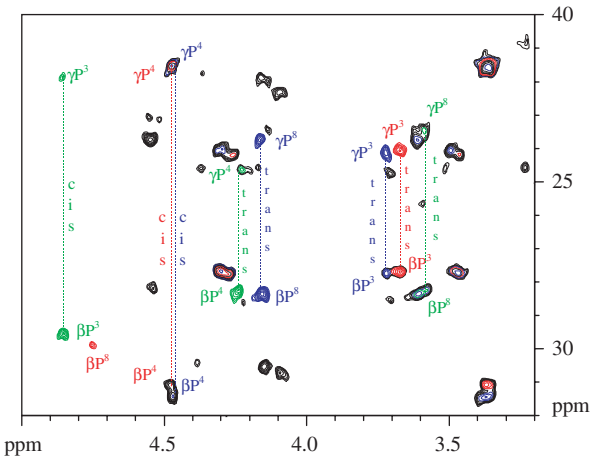

Figure 5 Portion of an HMQC-TOCSY spectrum at 600 MHz of a 6 mM solution of **YCKL** in DMSO-d_6, T = 298 K, τ_{mix} = 50 ms. The peaks are colour-coded as follows: blue, conformer I; red, conformer II; green, conformer III.

bond at position (i + 1, i + 2). An H-bond is not expected to form in such turns, and an H-bond was not found in the calculated structures, consistent with the high value of the temperature coefficient of Ser[7] NH for both peptides.

Comparison of the ϕ and ψ angles shows a similar behaviour for the two peptides. The ϕ angle of Trp[6]

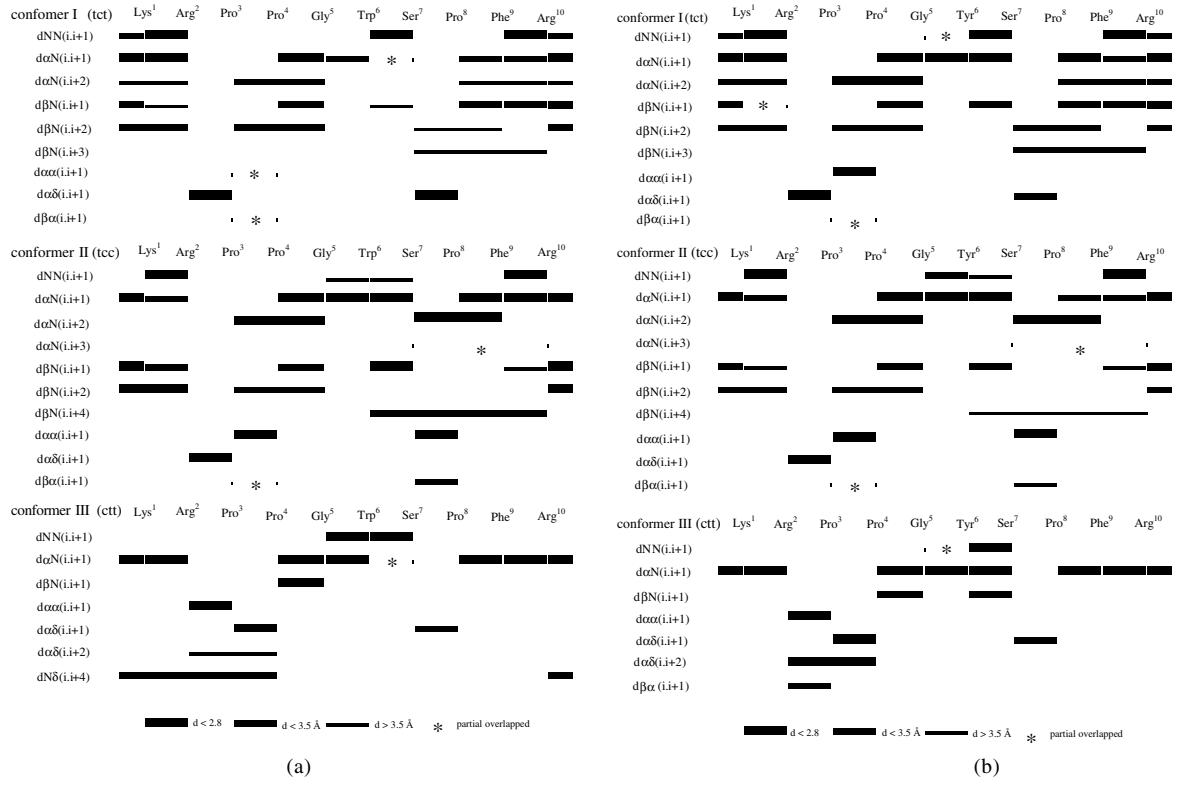

(a) (b)

Figure 6 (a) Summary of NOESY connectivities for the three conformers of **WCKL** in DMSO-d_6. Peaks are grouped into three classes based upon their integrated volumes. (b) Summary of NOESY connectivities for the three conformers of **YCKL** in DMSO-d_6. Peaks are grouped into three classes based upon their integrated volumes.

Table 6 Configuration of the X-Pro Bonds Determined for the Three Conformers of **WCKL** and **YCKL**

	Arg^2-Pro^3	Pro^3-Pro^4	Ser^7-Pro^8
I	*trans*	*cis*	*trans*
II	*trans*	*cis*	*cis*
III	*cis*	*trans*	*trans*

Table 7 Number of NOE Restraints Utilized in the Simulations for the Three Conformers of **WCKL** (**a**) and **YCKL** (**b**)

a

WCBK	i, i	i, i + 1	i, i + 2	i, i + 3	i, i + 4
I	32	32	8	1	0
II	54	30	4	1	3
III	24	16	1	0	1

b

YCBK	i, i	i, i + 1	i, i + 2	i, i + 3	i, i + 4
I	49	31	7	1	0
II	54	30	5	1	1
III	27	17	1	0	0

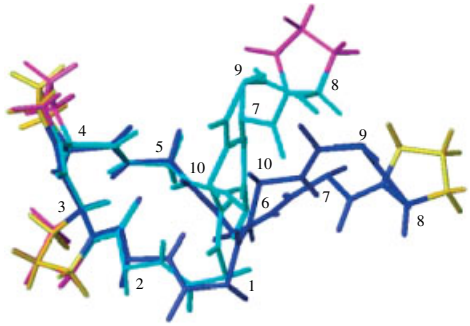

Figure 7 Overlay of representative structures for conformer I (*trans-cis-trans*) of the two peptides with the backbone atoms of residues 1–5 superimposed ($rmsd_{bb}$ = 1.18 Å). The lighter coloured chain is **WCKL**.

of **WCKL** shows a high dispersion with a very low order parameter and so do the ϕ angles of Ser^7 of both peptides.

The superposition of two representative structures for conformer II of the two peptides is reported in Figure 8.

Conformers III. 51 structures were analysed for **WCKL** and 50 for **YCKL**. The inter-residue NOE pattern for the two conformers is clearly poorer with respect to conformers I and II (see also Table 7). Only two medium range NOEs are present: $\alpha(2)$–$\delta(4)$ for both analogues

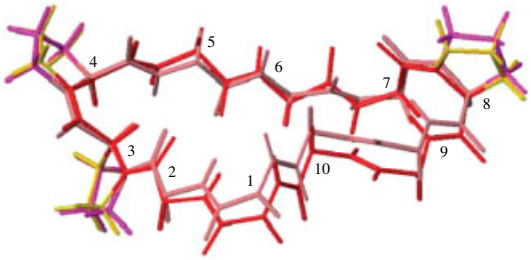

Figure 8 Overlay of representative structures for conformer II (*trans-cis-cis*) of the two peptides with the backbone atoms of residues 3, 4, 7 and 8 superimposed ($rmsd_{bb}$ = 0.39 Å). The lighter coloured chain is **WCKL**.

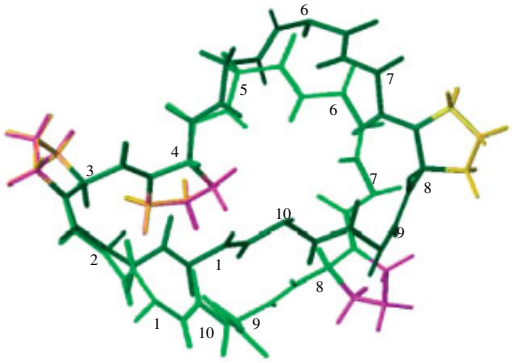

Figure 9 Overlay of representative structures for conformer III (*cis-trans-trans*) of the two peptides with the backbone atoms of residues 3 and 4 superimposed ($rmsd_{bb}$ = 1.50 Å). The lighter coloured chain is **WCKL**.

and Nδ(i,i + 4) between Arg^{10} and Pro^4 observed only for **WCKL**. From the analysis of backbone dihedral angles, no elements of secondary structure were found for this conformer of **WCKL**, while **YCKL** shows the possibility of a type-VIb β-turn between residues Arg^2 and Pro^3 and a polyproline II structure in position 3–4. The average backbone angles tables show a difference in ϕ value of Arg^2 and ψ value of Pro^4 between the two peptides. The overlay of two representative structures for conformer III of the two peptides is reported in Figure 9.

DISCUSSION

The conformational properties in DMSO of two linear analogues of **KL**, **YKL**, **WKL** and of their corresponding head-to-tail cyclic derivatives (**YCKL**, **WCKL**) were studied by NMR spectroscopy and distance geometry-simulated annealing calculations. All these peptides are B2 receptor agonists (Table 1). Substitution of only one residue, Phe^6, led to significant modification of biological activity. In the linear peptides, when Phe^6 is replaced by Trp the activity is increased, while when the Phe^6 is replaced by Tyr the activity is diminished. These data confirm that residue 6 plays a key role in the interaction with the B2 receptor. A number

Table 8 Average Backbone Dihedral Angles Calculated for the Three Conformers of **WCKL**: **a**, conformer I, averaged over 41 minimized structures unless otherwise indicated in parentheses, **b**, conformer II averaged over 45 minimized structures unless otherwise indicated in parentheses, **c**, conformer III, averaged over 51 minimized structures unless otherwise indicated in parentheses

Residue	ϕ	O.P.(ϕ)	ψ	O.P.(ψ)	Average global RMSD (Å) bb
a Conformer I					
Lys 1	-84.7 ± 14.6	0.969	-1.0 ± 11.2	0.982	1.73
Arg 2	-113.5 ± 42.8 (37)	0.633	144.8 ± 43.0	0.771	1.13
Pro 3	-76.5 ± 7.9		170.0 ± 8.0	0.991	1.48
Pro 4	-74.0 ± 1.8		154.6 ± 2.9	0.999	1.84
Gly 5	64.1 ± 65.0	0.535	153.0 ± 40.1	0.792	1.30
Trp 6	-75.4 ± 24.7	0.913	-13.3 ± 15.4	0.966	2.45
Ser 7	40.3 ± 82.4	0.412	150.9 ± 16.6	0.959	1.23
Pro 8	-83.6 ± 5.6		-44.7 ± 15.0	0.967	1.43
Phe 9	-101.6 ± 24.3	0.916	-1.1 ± 16.7	0.959	1.93
Arg 10	-156.2 ± 84.5	0.411	155.5 ± 18.0	0.952	0.87
b Conformer II					
Lys 1	-91.0 ± 9.5	0.987	-10.6 ± 9.0	0.988	0.50
Arg 2	-176.2 ± 5.7	0.995	146.6 ± 12.0	0.979	0.54
Pro 3	-83.7 ± 3.8		164.5 ± 3.1	0.999	0.65
Pro 4	-75.5 ± 1.5		130.8 ± 3.2	0.998	0.63
Gly 5	176.7 ± 15.6 (43)	0.879	179.8 ± 18.0 (43)	0.940	0.76
Trp 6	-97.0 ± 61.8	0.665	34.4 ± 5.6	0.995	1.04
Ser 7	-36.2 ± 77.8	0.388	149.7 ± 8.2	0.990	1.09
Pro 8	-90.9 ± 7.1		12.5 ± 16.2	0.962	1.26
Phe 9	-168.9 ± 37.1	0.817	46.5 ± 15.3	0.966	1.02
Arg 10	-73.5 ± 31.7	0.865	154.8 ± 3.3	0.998	0.48
c Conformer III					
Lys 1	29.5 ± 8.1	0.991	47.9 ± 8.2	0.990	0.42
Arg 2	-37.7 ± 2.5	0.999	139.3 ± 11.1	0.982	0.33
Pro 3	-86.1 ± 2.4		134.7 ± 1.9	0.999	0.28
Pro 4	-70.4 ± 1.9		179.2 ± 4.7	0.997	0.30
Gly 5	-170.1 ± 19.8	0.944	-1.5 ± 29.9	0.872	0.51
Trp 6	-134.0 ± 11.7	0.980	-67.2 ± 1.8	1.000	0.48
Ser 7	-92.4 ± 24.5	0.914	-166.5 ± 15.4	0.965	0.42
Pro 8	-77.8 ± 4.2		-178.7 ± 4.1	0.998	0.32
Phe 9	-26.6 ± 3.9	0.998	115.9 ± 8.1	0.990	0.25
Arg 10	-174.5 ± 8.1	0.990	144.9 ± 5.5	0.995	0.36

of model agonist–receptor complexes, based on the bacteriorhodopsin structure and on results from extensive site-directed mutagenesis of rhodopsin and other members of G-protein-coupled-receptor superfamily [13,68–70], have been reported in the literature. All these computationally derived models of bradykinin bound to the receptor retain a β-turn in the sequence 6–9, have variable conformations of the amino terminus and variable depths of insertion of the β-turn in the seven-helix bundle. In all these models, Phe^5 [46] and Phe^8 [13,46] side-chains (BK numbering notation) occupy a hydrophobic pocket between transmembrane helices of the receptor. In the case of kallidin, it is the aromatic residue in position 6 which has to be buried in this hydrophobic pocket. The results of our biological studies indicate that, among the aromatic residues, the indole side-chain of Trp seems to form stronger hydrophobic interactions than Phe or Tyr.

Our conformational studies on the two linear analogues reveal a high degree of conformational flexibility in DMSO. The predominant conformer, for both peptides, adopts a *trans* configuration at all the three X-Pro bonds; this conformer is not found in the corresponding cyclic analogues. The higher activity of the linear peptides would suggest that the active configuration is the all-*trans*. On the other hand, the *cis*/*trans* interconversion barrier of X-Pro bond in a linear peptide is about 20 kcal/mol and this value may

Table 9 Average Backbone Dihedral Angles Calculated for the Three Conformers of **YCKL**: **a** and **b**, conformer I and II, respectively, averaged over 43 minimized structures unless otherwise indicated in parentheses, **c**, conformer III averaged over 50 minimized structures unless otherwise indicated in parentheses

Residue	ϕ	O.P.(ϕ)	ψ	O.P.(ψ)	Average global RMSD (Å) bb
a Conformer I					
Lys 1	−84.8 ± 23.8	0.919	2.6 ± 19.0	0.948	1.41
Arg 2	−113.0 ± 27.9 (34)	0.510	151.8 ± 10.0	0.985	0.52
Pro 3	−76.5 ± 7.9		165.9 ± 4.8	0.997	0.70
Pro 4	−74.0 ± 1.8		152.0 ± 2.8	0.999	0.92
Gly 5	93.3 ± 20.4 (33)	0.691	124.0 ± 21.5 (33)	0.681	0.88
Tyr 6	−104.0 ± 17.4 (36)	0.665	34.4 ± 5.6	0.995	1.11
Ser 7	−54.4 ± 32.9	0.864	165.7 ± 8.9	0.988	0.62
Pro 8	−83.6 ± 5.6		−36.3 ± 8.8	0.988	0.66
Phe 9	−85.7 ± 7.6	0.991	10.6 ± 4.8	0.997	1.09
Arg 10	162.6 ± 3.0 (32)	0.572	102.4 ± 3.0	0.999	0.96
b Conformer II					
Lys 1	−96.5 ± 22.3	0.931	−6.3 ± 16.2	0.962	0.97
Arg 2	−164.5 ± 10.2	0.985	149.8 ± 7.5	0.992	0.60
Pro 3	−82.9 ± 6.2		167.9 ± 3.8	0.998	0.65
Pro 4	−78.0 ± 3.6		145.8 ± 3.3	0.998	0.67
Gly 5	133.8 ± 36.7	0.810	163.2 ± 37.2	0.808	0.79
Tyr 6	−136.3 ± 17.8	0.954	−178.1 ± 96.0	0.986	1.26
Ser 7	14.3 ± 84.9	0.352	151.4 ± 8.7	0.989	1.28
Pro 8	−91.6 ± 8.2		4.4 ± 9.4	0.987	1.30
Phe 9	−158.2 ± 29.5 (38)	0.756	33.2 ± 23.5	0.921	1.58
Arg 10	−85.2 ± 37.9	0.803	147.1 ± 12.0	0.979	0.72
c Conformer III					
Lys 1	−69.2 ± 31.8	0.877	177.8 ± 32.5	0.876	0.97
Arg 2	−91.3 ± 26.4	0.906	145.0 ± 5.7	0.995	0.60
Pro 3	−82.9 ± 6.2		137.5 ± 9.5	0.986	0.65
Pro 4	−78.0 ± 3.6		162.0 ± 1.8	1.000	0.67
Gly 5	−125.1 ± 15.4 (46)	0.843	−149.4 ± 4.4 (46)	0.943	0.79
Tyr 6	−94.6 ± 5.0	0.996	20.8 ± 1.8	1.000	1.26
Ser 7	−110.3 ± 13.0 (47)	0.930	154.9 ± 5.0 (47)	0.960	1.28
Pro 8	−91.6 ± 8.2		145.8 ± 40.0	0.777	1.30
Phe 9	48.8 ± 10.1 (48)	0.917	123.3 ± 48.9	0.696	1.58
Arg 10	−137.7 ± 63.1	0.562	141.2 ± 17.1	0.958	0.72

be low enough to allow interconversion *in vivo*, upon interaction with the receptor. The NMR results indicate that no significant secondary structure elements in solution are present in the all-*trans* conformers, in agreement with other published data [20,21,67]. However, these results are only in partial agreement with those of other previous investigations. Conformational studies carried out in various solvent media, such as DMSO, TFE, SDS micelles, revealed the presence of intramolecularly hydrogen bonded structures, involving either the *N*-terminal four residues [32,44] or the *C*-terminal residues [28,71]. Specifically, most of these studies proposed a β-turn (frequently type II) either in the segment 2–5, in 6–9 or in both the *C*- and the *N*-terminal part [23,72,73] as the dominant structural motif of peptide BK antagonists.

The present results do not allow us to describe a specific backbone conformation in the linear analogues. In DMSO, both linear peptides have the same conformational propensity, and the biological activity appears to depend on the presence of a specific amino acid residue in position 6 rather than on elements of secondary structure.

The results of a large number of structure–activity relationship studies have led to the general conclusion that the message sequence of kinin molecules could be located in the central amino acid sequence and that the peptide might bind the receptor in a quasi-cyclic form. Consequently, with the aim of stabilizing this putative bioactive conformation, several cyclic analogues of mammalian and insect kinins were synthesized: the cyclization either was head-to-tail

Table 10 Mean rmsd from Ideality for the Accepted Structures

	TCT		TCC		CTT	
	WCKL	YCKL	WCKL	YCKL	WCKL	YCKL
Bonds (Å)	0.008	0.008	0.01	0.008	0.008	0.006
Angles (deg)	0.95	0.91	0.97	0.87	0.94	0.76
Improper (deg)	0.66	0.46	0.50	0.42	0.33	0.15
NOEs (Å)	0.14	0.13	0.15	0.11	0.19	0.14

Mean energies (kcal/mol) for the accepted structures

	TCT		TCC		CTT	
	WCKL	YCKL	WCKL	YCKL	WCKL	YCKL
$E_{overall}$	139	137	185	112	140	80
E_{bond}	12	12	19	11	12	6
E_{angle}	46	40	47	37	44	28
E_{NOE}	73	81	112	58	79	43

[74,75] or involved the side chains [36,41]. In general, cyclization leads to modest agonistic or antagonistic activity, although in some cases a more potent peptide than the corresponding linear antagonist was obtained [23,42].

In our hands also, cyclization caused a marked reduction of receptor affinity. The biological test on rat duodenum showed that the cyclic peptide YCKL is 20 times less active than the corresponding linear YKL. Furthermore, cyclization of WKL, which was more potent than the corresponding linear KL, reduces the activity also with respect to YCKL. The rationalization of these biological results in terms of structure is no easy matter.

At least four conformers were present in each cyclic compound, differing in the *cis*/*trans* configuration at X-Pro bonds. It was possible to assign the complete sets of resonances for three of these conformers. The configurations at the X-Pro bonds are the same for the two analogues: conformer I and conformer II are in fast equilibrium, while conformer III does not exchange with the first two.

In our experimental conditions, all cyclic conformers show a *cis* configuration in at least one X-Pro bond and always opposite configuration for the two consecutive X-Pro bonds, possibly a consequence of the constraints of a ten amino acid cyclic structure. The interconversion around the Ser^7-Pro^8 bond is sufficiently slow on the NMR time scale to allow observation of exchange peaks between the first two conformers. Comparison of the NMR data through spectra analysis of the two analogues suggested that they are very similar. This was confirmed by structure calculations, except for conformer III.

In the low energy structures, the following elements of secondary structure were observed: a polyproline II structure in position 2–3 and a type I β-turn in position 8–9 for conformer I (*trans-cis-trans*), a type VI b β-turn in position 3–4 and a type VIa β-turn in position 7–8 for conformer II (*trans-cis-cis*). For the third conformer, a different result was found for the two analogues: no elements of structure in **WCKL**, and a type VIb β-turn in position 2–3 and a polyproline II structure in position 3–4 in **YCKL**. The results obtained in the present study indicate a conformational freedom within each of the conformers in solution and this could allow folding in a bioactive structure at the receptor binding site.

For the agonist cyclobradykinin, similar conformers to those found in the present study were described [44]. In the principal conformer, a β-turn is present in position Pro^8-Phe^9 (7–8 in BK numbering notation), exactly in the same position frequently reported in the literature for many active analogues of BK, both agonists and antagonists.

The *C*-terminal type I β-turn detected in conformer I was also found in a cyclic bradykinin mimic [67], although for linear antagonists and agonists a type II β-turn is usually observed [73,76–79]. Our data support the current hypothesis that this *C*-terminal turn is important in the receptor-bound conformation of the peptide. Indeed, the introduction of D-Tic-Oic [D-Tic, D-1,2,3,4-tetrahydroiso-quinoline-3-carboxylic acid; Oic, (S,S,S)-octahydroindole-2-carboxylic acid], designed to strengthen this β-turn, led to the most potent antagonist so far described (HOE-140) [45]. The existence of this β-turn in almost all the active analogues, in different solvent systems, strongly suggests that this

structural element is energetically stable, that it may be present in the receptor-bound state, and that it could be the structural requirement for receptor recognition and binding. In an attempt to explain the reduced activity of the two cyclic peptides with respect to that of the corresponding linear ones, it is reasonable to propose that cyclization leads to an unfavourable spatial arrangement of aromatic moieties within the receptor hydrophobic cluster.

REFERENCES

1. Bhoola KD, Figueroa CD, Worthy K. Bioregulation of kinins: kallikreins, kininogens, and kininases. *Pharmacol. Rev.* 1992; **44**: 1–80.
2. Stewart JM. Bradykinin antagonists: development and applications. *Biopolymers* 1995; **37**: 143–155.
3. Piek T. Neurotoxic kinins from wasp and ant venoms. *Toxicon* 1991; **29**: 139–149.
4. Comeau S, Lance VA, Hicks JW, Conlon JM. Purification and biological activity of alligator bradykinin. *Am. J. Physiol.* 1992; **263**: R400–R404.
5. Kimura M, Sueyoshi T, Takada K, Tanaka K, Morita T, Iwanaga S. Isolation and characterization of ornitho-kininogen. *Eur. J. Biochem.* 1987; **168**: 493–501.
6. Conlon JM, Le Mevel J-C, Conklin D, Weaver L, Duff DW, Olson KR. Isolation and cardiovascular activity of a second bradykinin-related peptide ([Arg^0, Trp^5, Leu^8]bradykinin) from trout. *Peptides* 1996; **17**: 531–537.
7. Regoli D, Barabe J. Pharmacology of bradykinin and related kinins. *Pharmacol. Rev.* 1980; **32**: 1–46.
8. Farmer SG, Burch RM. The pharmacology of bradykinin receptors. In *Bradykinin Antagonists: Basic and Clinical Research*, Burch RM (ed.). Marcel Dekker: New York, 1990; 1–31.
9. Kyle DJ, Burch RM. A survey of bradykinin receptors and their antagonists. *Curr. Opin. Invest. Drugs* 1993; **2**: 5–20.
10. Proud D, Reynolds CJ, Lacapra S, Kagey-Sobotka A, Lichtenstein LM, Naclerio RM. Nasal provocation with bradykinin induces symptoms of rhinitis and a sore throat. *Am. Rev. Respir. Dis.* 1988; **137**: 613–616.
11. Naclerio RM, Proud D, Lichtenstein LM, Kagey-Sobotka A, Hendley JO, Sorrentino J, Gwaltney JM. Kinins are generated during experimental rhinovirus colds. *J. Infect. Dis.* 1988; **157**: 133–142.
12. Regoli D, Rhaleb NE, Dion S, Drapeau G. New selective bradykinin receptor antagonists and bradykinin B2 receptor characterization. *Trends Pharmacol. Sci.* 1990; **11**: 156–161.
13. Jarnagin K, Bhakta S, Zuppan P, Yee C, Ho T, Phan T, Tahilramani R, Pease JHB, Miller A, Freedman R. Mutations in the B_2 bradykinin receptor reveal a different pattern of contacts for peptidic agonists and peptidic antagonists. *J. Biol. Chem.* 1996; **271**: 28 277–28 286.
14. Marceau F. Kinin B_1 receptors: a review. *Immunopharmacology* 1995; **30**: 1–26.
15. Salvino JM, Seoane PR, Dolle RE. Conformational analysis of bradykinin by annealed molecular dynamics and comparison to NMR-derived conformations. *J. Comput. Chem.* 1993; **14**: 438–444.
16. Chipens GI, Mutulis FK, Katayev BS, Klusha VE, Misina IP, Myshlyiakova NV. Cyclic analogue of bradykinin possessing selective and prolonged biological activity. *Int. J. Peptide Protein Res.* 1981; **18**: 302–311.
17. Perez JJ, Sanchez YM, Centeno NB. Characterization of the conformational domains of bradykinin by computational methods. *J. Peptide Sci.* 1995; **1**: 227–235.
18. Deslauriers R, Komoroski RA, Levy GC, Paiva ACM, Smith ICP. Conformational heterogeneity in linear peptides in solution: a carbon-13 NMR study of [Pro^3, Pro^5]-angiotensin-II. *FEBS Lett.* 1976; **62**: 50–56.
19. Kyle DJ, Martin JA, Farmer SG, Burch RM. Design and conformational analysis of several highly potent bradykinin receptor antagonists. *J. Med. Chem.* 1991; **34**: 1230–1233.
20. Denys L, Bothner-By AA, Fisher GH, Ryan JW. Conformational diversity of bradykinin in aqueous solution. *Biochemistry* 1982; **21**: 6531–6536.
21. London RE, Stewart JM, Cann JR, Matwiyoff NA. ^{13}C and ^{1}H nuclear magnetic resonance studies of bradykinin and selected peptide fragments. *Biochemistry* 1978; **17**: 2270–2277.
22. Saulitis JB, Liepins EE, Sekacis IP, Mutulis FK, Chipens GI. 2D NMR spectroscopy study of the spatial structure of kinins: Bradykinin, kallidin and their cyclic analogs. In *Peptides: Chem. Struct. Biol.* Proceeding of the 11th American Peptide Symposium, Rivier JE, Marshall GR (eds). ESCOM: Leiden, 1990; 588–589.
23. Krause K, Pineda LF, Peteranderl R, Reissmann S. Conformational properties of cyclic peptide bradykinin B_2 receptor antagonist using experimental and theoretical methods. *J. Peptide Res.* 2000; **55**: 63–71.
24. Monteagudo ES, Calvani F, Catrambone F, Fincham CI, Madami A, Meini S, Terracciano R. New conformationally homogeneous β-turn antagonists of the human B_2 kinin receptor. *J. Peptide Sci.* 2001; **7**: 270–283.
25. Mirmira SR, Durani S, Srivastava S, Phadke RS. Occurrence of β-bends in bradykinin dissolved in DMSO-d_6. *Magn. Reson. Chem.* 1990; **28**: 587–593.
26. Pellegrini M, Gobbo M, Rocchi R, Peggion E, Mammi S, Mierke DF. Threonine^6-bradykinin: conformational study of a flexible peptide in dimethyl sulfoxide by NMR and ensemble calculations. *Biopolymers (Pept. Sci.)* 1997; **40**: 561–569.
27. Young JK, Hicks RP. NMR and molecular modeling investigations of the neuropeptide bradykinin in three different solvent systems: DMSO, 9:1 dioxane/water, and in the presence of 7.4 mM lyso phosphatidylcholine micelles. *Biopolymers* 1994; **34**: 611–623.
28. Lee SC, Russell AF, Laidig WD. Three-dimensional structure of bradykinin in SDS micelles. *Int. J. Peptide Protein Res.* 1990; **35**: 367–377.
29. Pellegrini M, Mammi S, Peggion E, Mierke DF. Threonine^6-bradykinin: structural characterization in the presence of micelles by nuclear magnetic resonance and distance geometry. *J. Med. Chem.* 1997; **40**: 92–98.
30. Pellegrini M, Mierke DF. Threonine^6-bradykinin: molecular dynamics simulations in a biphasic membrane mimetics. *J. Med. Chem.* 1997; **40**: 99–104.
31. Kyle DJ, Hicks RP, Blake PR, Klimkowski VJ. Conformational properties of bradykinin and bradykinin antagonists. In *Bradykinin Antagonists: Basic and Clinical Research*, Burch RM (ed.). Marcel Dekker: New York, 1990; 131–146.
32. Cann JR, Liu X, Stewart JM, Gera L, Kotovych G. A CD and an NMR study of multiple bradykinin conformations in aqueous trifluoroethanol solutions. *Biopolymers* 1994; **34**: 869–878.
33. Miskolzie M, Gera L, Stewart JM, Kotovych G. The importance of the *N*-terminal β-turn in bradykinin antagonists. *J. Biomol. Struct. Dyn.* 2000; **18**: 249–260.
34. Pellegrini M, Tancredi M, Rovero P, Mierke DF. Probing the topological arrangement of the *N*- and *C*-terminal residues of bradykinin for agonist activity at the B1 receptor. *J. Med. Chem.* 1999; **42**: 3369–3377.
35. Mutulis FK, Chipens GI, Lando OE, Mutule IE. Cyclic analogues of bradykinin. II. Synthesis of cyclic derivatives of kallidin. *Int. J. Peptide Protein Res.* 1984; **23**: 235–241.
36. Chipens GI, Mutulis FK, Myshlyakova NV, Misina IP, Vitolina RO, Klusha VJ, Katayev BS. Cyclic analogues of bradykinin. *Int. J. Peptide Protein Res.* 1985; **26**: 460–468.
37. Gobbo M, Biondi L, Filira F, Rocchi R, Piek T. Synthesis and biological activity of some linear and cyclic kinin analogues. *Int. J. Peptide Protein Res.* 1994; **44**: 1–9.

38. Gobbo M, Biondi L, Filira F, Rocchi R, Mantel P, van Weeren-Kramer J, Piek T. Linear and cyclic Tyr^6- and Trp^6-kallidin (Lys-bradykinin) analogues. *Gazzetta Chim. Ital.* 1996; **126**: 259–363.
39. Gobbo M, Biondi L, Cavaggion F, Filira F, Piek T, Mantel P, Rocchi R. Synthesis and biological activities of head-to-tail cyclic bradykinin analogues of varying ring size. *Int. J. Peptide Protein Res.* 1997; **50**: 336–341.
40. Gobbo M, Biondi L, Filira F, Rocchi R, Piek T. On the role of basic residues of head-to-tail cyclic bradykinin analogues on rat duodenum relaxation. *Lett. Peptide Sci.* 2000; **7**: 171–178.
41. Seyfarth L, Pineda de Castro LF, Liepina I, Paegelow I, Liebmann C, Reissmann S. New cyclic bradykinin antagonists containing disulfide and lactam bridges at the N-terminal sequence. *Int. J. Peptide Protein Res.* 1995; **46**: 155–165.
42. Schumann C, Seyfarth L, Greiner G, Paegelow I, Reissmann S. Synthesis and biological activities of new side chain and backbone cyclic bradykinin analogues. *J. Peptide Res.* 2002; **60**: 128–140.
43. Piek T, Rocchi R, Hue B. Neurotoxic actions of kinins — a contribution to the localization of the pharmacophore. *Toxicon* 1994; **32**: 389.
44. Pellegrini M, Mammi S, Gobbo M, Rocchi R, Peggion E. Conformation of cyclobradykinin by NMR and distance geometry calculations. *Biopolymers* 1995; **36**: 461–472.
45. Hock FJ, Wirth K, Albus U, Linz W, Gerhards HJ, Wiemer G, Henke S, Breipohl G, König W, Knolle J, Schölkens BA. Hoe 140 a new potent and long acting bradykinin-antagonist: *in vitro* studies. *Br. J. Pharmacol.* 1991; **102**: 769–773.
46. Kyle DJ, Chakravarty S, Sinsko JA, Stormann TM. A proposed model of bradykinin bound to the rat B2 receptor and its utility for drug design. *J. Med. Chem.* 1994; **37**: 1347–1354.
47. Derome AE, Williamson MP. Rapid-pulsing artifacts in double-quantum-filtered COSY. *J. Magn. Reson.* 1990; **88**: 177–185.
48. Bax A, Davis DG. MLEV-17-Based Two-dimensional homonuclear magnetization transfer spectroscopy. *J. Magn. Reson.* 1985; **65**: 355–360.
49. Griesinger C, Otting G, Wüthrich K, Ernst RR. Clean TOCSY for ^1H spin system identification in macromolecules. *J. Am. Chem. Soc.* 1988; **110**: 7870–7872.
50. Kumar A, Ernst RR, Wüthrich K. A two-dimensional nuclear Overhauser enhancement (2D NOE) experiment for the elucidation of complete proton-proton cross-relaxation networks in biological macromolecules. *Biochem. Biophys. Res. Commun.* 1980; **95**: 1–6.
51. Macura S, Huang Y, Suter D, Ernst RR. Two-dimensional chemical exchange and cross-relaxation spectroscopy of coupled nuclear spins. *J. Magn. Reson.* 1981; **43**: 259–281.
52. Bax A, Davis DG. Practical aspects of two-dimensional transverse NOE spectroscopy. *J. Magn. Reson.* 1985; **63**: 207–213.
53. Drobny G, Pines A, Sinton S, Weitekamp DP, Wemmer D. Fourier transform multiple quantum nuclear magnetic resonance. *Faraday Symp. Chem. Soc.* 1979; **13**: 49–55.
54. Bodenhausen G, Vold RL, Vold RR. Multiple quantum spin-echo spectroscopy. *J. Magn. Reson.* 1980; **37**: 93–106.
55. Wüthrich K. *NMR of Protein and Nucleic Acids*. John Wiley and Sons: New York, 1986; 130–161.
56. Lerner L, Bax A. Sensitivity-enhanced two-dimen-sional heteronuclear relayed coherence transfer NMR spectroscopy. *J. Magn. Reson.* 1986; **69**: 375–380.
57. Bax A, Subramanian S. Sensitivity-enhanced two-dimensional heteronuclear shift correlation NMR spectroscopy. *J. Magn. Reson.* 1986; **67**: 565–569.
58. Shaka AJ, Barker PB, Freeman R. Computer-optimized decoupling scheme for wideband applications and low-level operation. *J. Magn. Reson.* 1985; **64**: 547–552.
59. Neidig K-P, Geyer M, Görler A, Antz C, Saffrich R, Beneicke W, Kalbitzer HR. AURELIA, a program for computer-aided analysis of multi-dimensional NMR spectra. *J. Biomol. NMR* 1995; **6**: 255–270.
60. Wüthrich K, Billeter M, Braun W. Pseudo-structures for the 20 common amino acids for use in studies of protein conformations by measurements of intramolecular proton-proton distance constraints with nuclear magnetic resonance. *J. Mol. Biol.* 1983; **169**: 949–961.
61. Brunger AT. *XPLOR Version 3.0: A System for X-ray Crystallography and NMR*. Yale University Press: New Haven, 1992.
62. Koradi R, Billeter M, Wüthrich K. MOLMOL: a program for display and analysis of macromolecular structures. *J. Mol. Graphics* 1996; **14**: 51–55, 29–32.
63. Deber CM, Madison V, Blout ER. Why cyclic peptides? Complementary approaches to conformations. *Acc. Chem. Res.* 1976; **9**: 106–113.
64. Kessler H. Conformation and biological activity of cyclic peptides. *Angew. Chem. Int. Ed. Engl.* 1982; **21**: 512–523.
65. Lee W, Krishna NR. Influence of conformational exchange on the 2D NOESY spectra of biomolecules existing in multiple conformations. *J. Magn. Reson.* 1992; **98**: 36–48.
66. Hyberts SG, Goldberg MS, Havel TF, Wagner G. The solution structure of eglin c based on measurements of many NOEs and coupling constants and its comparison with x-ray structures. *Protein Sci.* 1992; **1**: 736–751.
67. Miskolzie M, Yamamoto H, York EJ, Stewart JM, Kotovych G. An NMR conformational analysis of cyclic bradykinin mimics. Evidence for a β-turn. *J. Biomol. Struct. Dyn.* 2000; **17**: 947–955.
68. Hibert MF, Trumpp-Kallmeyer S, Bruinvels A, Hoflack J. Three-dimensional models of neurotransmitter G-binding protein-coupled receptors. *Mol. Pharmacol.* 1991; **40**: 8–15.
69. Strader CD, Fong TM, Tota MR, Underwood D, Dixon RA. Structure and function of G protein-coupled receptors. *Annu. Rev. Biochem.* 1994; **63**: 101–132.
70. Nathans J. Rhodopsin: structure, function, and genetics. *Biochemistry* 1992; **31**: 4923–4931.
71. Cann JR, Stewart JM, Matsueda GR. A circular dichroism study of the secondary structure of bradykinin. *Biochemistry* 1973; **12**: 3780–3788.
72. Ivanov VT, Filatova MP, Reissmann S, Rentova TO, Efremov ES, Pashkov VS, Galaktionov SG, Grigoryan GL, Ovchinnikov YuA. The solution conformation of bradykinin. In *Peptides: Chemistry, Structure and Biology. Proceedings of the Fourth American Peptide Symposium*, Walter R, Meienhofer J (eds). Ann Arbor Science Publishers: Ann Arbor, 1975; 151–157.
73. Sejbal J, Cann JR, Stewart JM, Gera L, Kotovych G. An NMR, CD, Molecular dynamics, and fluorometric study of the conformation of the bradykinin antagonist B-9340 in water and in aqueous micellar solutions. *J. Med. Chem.* 1996; **39**: 1281–1292.
74. Saulitis J, Liepins E, Mutulis F, Chipens G. Interpretation of the proton NMR spectra of a cyclic analog of kallidin in solution. *Bioorg. Khim.* 1986; **12**: 1317–1328.
75. Krstenansky JL, Ho T, Tahilramani R, Pease JHB, Bhakta S, Ostrelich H, Jarnagin K. Cyclic hexapeptide antagonists of the bradykinin B_2 receptor: Receptor binding and solution backbone conformation. *Lett. Peptide Sci.* 1994; **1**: 229–234.
76. Guba W, Haessner R, Breipohl G, Henke S, Knolle J, Santagada V, Kessler H. Combined approach of NMR and molecular dynamics within a biphasic membrane mimetic: conformation and orientation of the bradykinin antagonist Hoe 140. *J. Am. Chem. Soc.* 1994; **116**: 7532–7540.
77. Sejbal J, Wang Y, Cann JR, Stewart JM, Gera L, Kotovych G. A comparative NMR and molecular dynamics study of the conformations of bradykinin B1 and B2, B2, and B1-specific receptor antagonists B-9430, B-9436, and B-9858. *Biopolymers* 1997; **42**: 521–535.
78. Kotovych G, Cann JR, Stewart JM, Yamamoto H. NMR and CD conformational studies of bradykinin and its agonists and antagonists: application to receptor binding. *Biochem. Cell Biol.* 1998; **76**: 257–266.
79. Kyle DJ, Blake PR, Smithwick D, Green LM, Martin JA, Sinsko JA, Summers MF. NMR and computational evidence that high-affinity bradykinin receptor antagonists adopt *C*-terminal β-turns. *J. Med. Chem.* 1993; **36**: 1450–1460.

